

General Relativistic Radiative Transfer

Sebastian Knop^{1,2}, Peter H. Hauschildt¹, and E. Baron²

¹ Hamburger Sternwarte, Gojenbergsweg 112, 21029 Hamburg, Germany

² University of Oklahoma, 440 West Brooks, Rm 100, Norman, OK 73019-2061, USA

Received date Accepted date

ABSTRACT

Aims. We present a general method to calculate radiative transfer including scattering in the continuum as well as in lines in spherically symmetric systems that are influenced by the effects of general relativity (GR). We utilize a comoving wavelength ansatz that allows to resolve spectral lines throughout the atmosphere.

Methods. The used numerical solution is an operator splitting (OS) technique that uses a characteristic formal solution. The bending of photon paths and the wavelength shifts due to the effects of GR are fully taken into account, as is the treatment of image generation in a curved spacetime.

Results. We describe the algorithm we use and demonstrate the effects of GR on the radiative transport of a two level atom line in a neutron star like atmosphere for various combinations of continuous and line scattering coefficients. In addition, we present grey continuum models and discuss the effects of different scattering albedos on the emergent spectra and the determination of effective temperatures and radii of neutron star atmospheres.

Key words. Radiative transfer – Relativity – Scattering

1. Introduction

In the last few decades much effort has been put into the modeling of radiative transfer in relativistically moving atmospheres such as novae and supernovae. One of the state of the art techniques to solve this problem is the operator splitting (OS) method. This method has been successfully used to solve radiative transfer problems with scattering and complete treatment of non-local thermodynamic equilibrium (NLTE) effects.

However, these sophisticated methods for treating radiative transfer have not been used in a general relativistic environment, although the form of the GR equation of transfer does, basically, not differ from the special relativistic version and the OS method can be applied to such problems.

There have been several successful attempts to model the emergent spectra of general relativistic systems such as neutron stars. These models also account for magnetic fields or different surface temper-

atures. However, the radiative transfer in these cases generally solves classical plane parallel problems. See Zavlin & Pavlov (2002) for a review.

Here we present an OS method of solving GR radiative transfer problems in spherical (Schwarzschild) geometry. Other authors have solved the radiative transfer problem in GR. For instance Schinder & Bludman (1989) solve the moment equations of radiative transfer with a variable Eddington factor method. The advantage of OS is not only that it does not depend on closure conditions but can also solve magneto-optical transfer, what could prove to be important as far as neutron stars are concerned.

Zane et al. (1996) developed a characteristics method to solve general relativistic radiative transport problems. They utilize the constants of motion for the description of photon orbits that arise due to the Killing vectors of the spherically symmetric spacetime and use the analytical connection of an affine parameter with the radial coordinate as

well as choosing the momentum variables along the characteristics to be constant to formulate the radiative transport equation. Although this simplifies the equation in the case of flows such as accretion onto black holes and neutron stars, the lack of a comoving wavelength description forces the use of a large number of characteristics to resolve the (in this case) angular dependent absorption coefficients and a huge number of wavelength points to resolve the shift of spectral lines through the atmosphere. The latter is necessary even in the case of static general relativistic atmospheres, e.g., in neutron stars.

We avoid these problems by using a comoving wavelength coordinate which explicitly accounts for the coupling of different wavelengths. This ansatz is the important core part of this work. Since in order to calculate detailed spectra you need to resolve spectral lines throughout the atmosphere and you cannot afford to use a wavelength description that depends on the layer of the atmosphere that you are at. Since in order to perform NLTE calculations you would have to add a significant number of wavelengths to your computation to resolve the spectral line at hand in every layer with the desired quality.

In the following we present calculations of general relativistic radiative line and continuum transfer with a complete treatment of scattering. In order to demonstrate the functionality of the method, we chose a simple test case similar to a neutron star atmosphere.

2. Radiative Transfer

Lindquist found the equation for radiative transfer for a comoving metric (Lindquist, 1966). He used the photon distribution function as variable to describe the radiation field. The works of Schinder & Bludman (1989) and Zane et al. (1996) follow this ansatz.

However, we want to utilize a description of the radiation via the specific intensity that is suitable for our method of solution.

Rather than using the general metric used by Lindquist, we neglect the effects of the atmosphere on the metric and use the Schwarzschild solution:

$$g_{\alpha\beta} = \begin{pmatrix} 1 - \frac{2MG}{c^2 r} & 0 & 0 & 0 \\ 0 & -\frac{1}{1 - \frac{2MG}{c^2 r}} & 0 & 0 \\ 0 & 0 & -r^2 & 0 \\ 0 & 0 & 0 & -r^2 \sin^2 \Theta \end{pmatrix}. \quad (1)$$

Since the atmospheres that are influenced by GR effects typically have a small mass compared to the parent object, this simplification is well justified. Furthermore, it is possible to calculate the metric coefficients for spherical symmetry by integrating the Tolman-Oppenheimer-Volkov equations and thus avoiding this approximation if desired.

The equation of radiative transfer in the Schwarzschild metric is then found in its characteristic form:

$$\frac{\partial I_\lambda}{\partial s} + a_\lambda \frac{\partial \mathcal{I}_\lambda}{\partial \lambda} + 4a_\lambda I_\lambda = \eta_\lambda - \chi_\lambda I_\lambda \quad (2)$$

with

$$\frac{\partial}{\partial s} = \frac{\partial r}{\partial s} \frac{\partial}{\partial r} + \frac{\partial \mu}{\partial s} \frac{\partial}{\partial \mu} \quad (3)$$

$$\frac{\partial r}{\partial s} = \sqrt{1 - \frac{2MG}{c^2 r}} \mu \quad (4)$$

$$\frac{\partial \mu}{\partial s} = \frac{1 - \mu^2}{r} \left(1 - \frac{MG}{c^2 r - 2MG} \right) \sqrt{1 - \frac{2MG}{c^2 r}} \quad (5)$$

$$a_\lambda = \sqrt{\frac{r}{r - \frac{2MG}{c^2}}} \frac{MG}{c^2 r^2} \mu \quad (6)$$

This development is equivalent to the work of Lindquist and delivers no new physical insight besides being in the same form as the spherically symmetric special relativistic equation of transfer (Mihalas, 1980). Hence modern operator splitting techniques to solve radiative transfer are applicable to the problem.

However, there is a fundamental difference from the special relativistic equation of transfer. The coefficient a_λ does not change sign in monotonic flows that describe, e.g., supernova and nova atmospheres. In the GR case, this coefficient is linear in μ and hence the sign of a_λ will be different for ingoing ($\mu < 0$) and outgoing ($\mu > 0$) photons. a_λ couples different wavelengths and determines how the spectral features shift due to the flow or the gravitational field. In the case of a supernova atmosphere the different parts of the atmosphere all move away from each other so that the direction of the wavelength shift along a ray is always the same, hence a_λ has the same sign along the ray. In a gravitational field, ingoing photons will be blueshifted and outgoing photons will be redshifted and hence, the sign of a_λ changes. This presents a difficulty as the direction of flow of information in the wavelength space

is reversed along a ray and the transfer equation is no longer an initial value problem in wavelength space, but a 2-point boundary value problem.

Mihalas already realized this in Mihalas (1980) and outlined a simple ray by ray formal solution to this problem. However, this solution is of little use for the construction of an approximate Λ -operator for an ALI-iteration. To solve this problem we use the OS method described in detail in Baron & Hauschildt (2004).

The treatment of arbitrarily flows of information in the wavelengthspace means that every spatial point at all wavelengths can influence the intensity at a given spatial point at a given wavelength. This forces you to use a matrix notation for the formal solution where you have to implement proper boundary conditions governed by a_λ at every spatial point for all wavelengths to ensure a locally stable upwind scheme for the wavelength discretization.

The GR case is a rather simple application to this method since the flow of information in the wavelengthspace just changes once on a ray, namely at the point of tangency or in the case of core intersecting rays at the innermost layer.

To make this method work with the GR case you have to calculate a_λ for every wavelength on all points of a given characteristic and determine the appropriate discretization of the derivative at this point. Furthermore you have to know the pathlength between two neighboring points on a ray to be able to calculate the change of optical depth along the ray for all wavelengths. In addition to that you must determine the angles of intersection with a given layer for all characteristics in order to perform angular integrations.

A photon in a gravitational field not only experiences a wavelength shift but also is deflected since it moves on a null-geodesic for the given spacetime. Since we are employing a characteristics based solution we can fully account for this effect. The spatial derivatives in equation (2) describe the geometry of our characteristics. They are still geodesics and can be described by an affine parameter.

In order to obtain the rays, the $\frac{\partial}{\partial s}$ part of equation (2) has to be integrated. For the Schwarzschild metric it is possible to analytically describe the photon orbits in terms of constants of the motion. In addition, we have to relate the affine parameter to the distance along the characteristics. In the one dimensional case, the integration is simple and fast. Since

the spacetime just outside the atmosphere will, in general, not be flat, we extend our calculation of the characteristics into a regime of spacetime that can be considered flat – in our test calculations discussed below, we chose a boundary of ten Schwarzschild-radii – to make sure that we calculate the spectrum from a correct set of angles that represent the imaging of the source in curved spacetime.

We assume vacuum conditions outside the atmosphere and, therefore, the intensities will not change along the characteristic outside the atmosphere, of course except for being redshifted due to the gravitational field what is trivial to account for.

3. The Testing Setup

We solve the test radiative transfer problems in a spherical model configuration with 50 radial points (layers). We assume an exponential density structure

$$\varrho(r) = \varrho_0 \exp \frac{r - r_{\text{out}}}{r_{\text{scale}}} \quad (7)$$

within the atmosphere and that the gas consists only of a simple two-level-atom with a wavelength independent background continuum.

For a given optical depth (τ) grid we integrate the radial grid via

$$\frac{dr}{d\tau} = -\frac{1}{\chi_\kappa} \quad (8)$$

where $\chi_\kappa = \chi_0 \varrho(r)$ with ϱ given by (7). It should be noted that χ_κ represents only the continuum extinction coefficient. The resulting structure is not intended to be an accurate model of a neutron star atmosphere. However, it has the correct spatial dimensions and we thus use it to make predictions how GR will affect radiative transfer in a realistic neutron star atmosphere.

In Fig. 1 we plot the radial structure of the test atmosphere versus the optical depth grid that we used for the calculations in section 4. The method of Baron & Hauschildt (2004) makes it necessary to provide a spatial boundary condition for the characteristics which is done via the diffusion approximation. We generate a simple grey temperature structure with the Hopf-function (Chandrasekhar, 1950). To describe the single spectral line of the two-level-atom, we define a wavelength λ_{line} as the center of

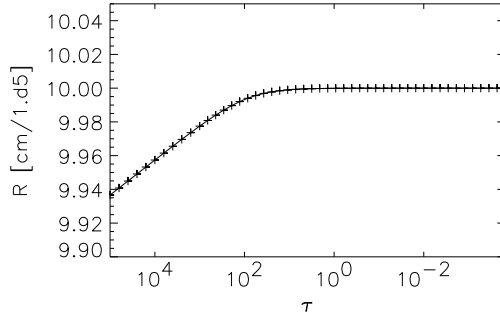


Fig. 1. Radius is plotted over optical depth. The optical depth was calculated from the wavelength independent continuous opacity. The atmosphere is about 60 meters thick, but the layers with an optical depth around one lie just centimeters below the outermost layer.

the line and use a Gaussian profile centered on this wavelength:

$$\Phi(\lambda) = \frac{\omega_{\text{line}}}{\sqrt{\pi}} \exp\left(-\frac{\lambda - \lambda_{\text{line}}}{\omega_{\text{line}}}\right)^2, \quad (9)$$

with ω_{line} being the width of the Gaussian. We describe the opacity associated with the line via:

$$\chi_{\text{line}}(\tau, \lambda) = \chi_{\kappa}(\tau) R_{\text{line}} \frac{\Phi(\lambda)}{\int \Phi(\lambda) d\lambda}, \quad (10)$$

whereby the R_{line} factor determines the strength of the line relative to the continuum.

It should be noted that the Gaussian width of the line is only 0.01 \AA . This is very small and does not represent a line width one would expect in neutron star atmosphere due to the large temperatures and pressures present in such an atmosphere. The small width was chosen to highlight the effects of GR on radiative transfer. Since the atmosphere of a neutron star is only a few centimeters thick, the intrinsic wavelength shifts within the atmosphere are very small and the GR effects can be tested best with very narrow lines.

A detailed treatment of radiative transfer especially in the general relativistic environment of a neutron star atmosphere is desirable, since constraints on the mass-radius relation are needed for the understanding of neutron star interiors and its

equation of state. The constraint should be as strict as possible and, therefore, the radiative transfer should be as sophisticated as possible.

Realistic models will need a multidimensional description and have characteristics in the atmosphere that extend over larger portions of space-time and hence have a larger intrinsic wavelength shift. Furthermore there may be configurations of blended lines that create a rapidly changing opacity as seen, e.g., in the UV spectra of classical novae (Hauschildt et al., 1995).

Furthermore, in realistic models of accretion columns on neutron stars the atmosphere extends over larger regions of spacetime and the intrinsic line shifts will be much larger. Therefore, there are physical systems where you expect, that detailed general relativistic radiative transfer is important. Besides this method is not limited to static atmospheres but can also be applied to gamma-ray-bursts, accretion scenarios, or neutrino transport in early phases of core collapse supernovae.

Since we treat the radiative transfer problem with scattering, we need to specify the quantities ϵ_{κ} and ϵ_{line} to define the scattering albedo. The true absorption and the scattering part of the continuum opacity can now be expressed through:

$$\kappa_{\kappa}(\tau) = \epsilon_{\kappa} \chi_{\kappa}(\tau) \quad (11)$$

$$\sigma_{\kappa}(\tau) = (1 - \epsilon_{\kappa}) \chi_{\kappa}(\tau) \quad , \quad (12)$$

whereas for the line opacity we have:

$$\kappa_{\text{line}}(\tau, \lambda) = \epsilon_{\text{line}} \chi_{\text{line}}(\tau, \lambda) \quad (13)$$

$$\sigma_{\text{line}}(\tau, \lambda) = (1 - \epsilon_{\text{line}}) \chi_{\text{line}}(\tau, \lambda) \quad . \quad (14)$$

The total opacity can now be given as:

$$\chi_{\text{total}}(\tau, \lambda) = \kappa_{\kappa}(\tau) + \sigma_{\kappa}(\tau) + \kappa_{\text{line}}(\tau, \lambda) + \sigma_{\text{line}}(\tau, \lambda) \quad (15)$$

while the emissivity is:

$$\eta_{\text{total}}(\tau, \lambda) = (\kappa_{\kappa}(\tau) + \kappa_{\text{line}}(\tau, \lambda)) B(T(\tau)) + (\sigma_{\kappa}(\tau) + \sigma_{\text{line}}(\tau, \lambda)) J(\tau, \lambda). \quad (16)$$

Note that the continuous opacity is constant over the wavelength range of interest and that the scattering was assumed to be coherent for simplicity.

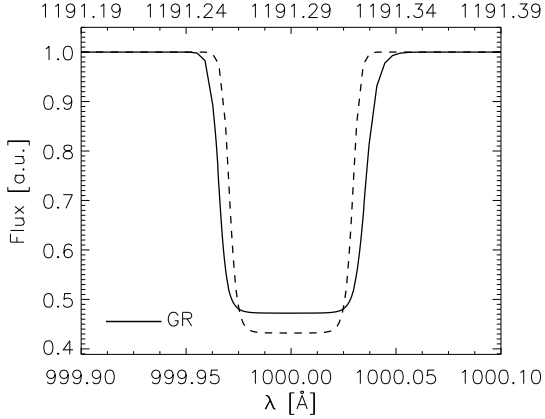


Fig. 2. Results for non-scattering model line and continuum.

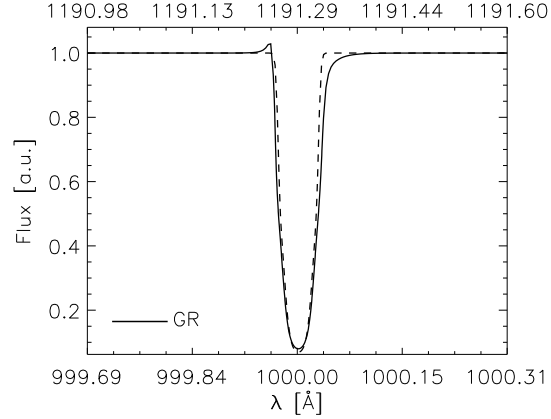


Fig. 3. The model line and the continuum are scattering with $\epsilon_{\text{line}} = 0.01$ and $\epsilon_{\kappa} = 0.01$ respectively.

4. Results

We calculate the emerging spectra of the model line for various combinations of scattering parameters for the continuum and for the line – hence providing a NLTE treatment of the line transfer. In Figs. 2 to 6 we always show two cases with different gravitational masses – one with $M = 0$ and the other with $M = M_{\odot}$. The wavelength scale at the bottom corresponds to the massless case and the upper scale to the one solar mass case. The emerging line profiles are plotted over each other in order to be easily compared. All calculated spectra include the full treatment of scattering unless it is indicated that a scattering parameter was set to one.

We include the massless case in order to verify the code by comparing the results to the thoroughly tested special relativistic code and obtained the same results with both methods. In addition, all other tests such as omitting the line and recovering a flat continuum for constant thermal sources, sudden changes in the wavelength resolution, and wavelength dependent boundary conditions produced correct results.

In Fig. 2 the continuum as well as the line are purely thermal. In the massless case this results in a symmetric absorption line while in the general relativistic case for one solar mass the line profile deforms and becomes asymmetric with an extended wing to the red, although the effect is very small. The line profiles are normalized to the continuum

and the equivalent widths of the two lines are different. Although the radial structure and the run of the opacities is exactly the same in both cases, the effective opacity is different. due to the factor $4a_{\lambda}$ in equation 2.

In Fig. 3 the line and the continuum are scattering with $\epsilon_{\text{line}} = 0.01$ and $\epsilon_{\kappa} = 0.01$. In the massless case this results in a symmetric absorption profile with line wings slightly in emission, while in the general relativistic case the line profile is very asymmetric with an emission feature on the blue side and an extended red absorption wing.

The model parameters used to generate Fig. 4 resemble those of Fig. 3. The only difference is a stronger scattering in the continuum $\epsilon_{\kappa} = 1.0 \times 10^{-6}$. The strength and shape of the blue emission depends on the scattering in the continuum. For a strong scattering continuum even in the massless case an emission feature appears in both wings of the line. It can be explained with the Schuster-mechanism (Mihalas, 1978). In the relativistic case this mechanism appears to be amplified and strongly distorted in the red wing. To rule out any effect of line scattering, we have calculated a model line with pure scattering ($\epsilon_{\kappa} = 0$) in the continuum and no scattering in the line. The result is shown in Fig. 5. The massless case shows the expected absorption profile with the wings in emission. In the relativistic case, the shape of the blue emission feature does not change compared to the cases with less scattering. However, its

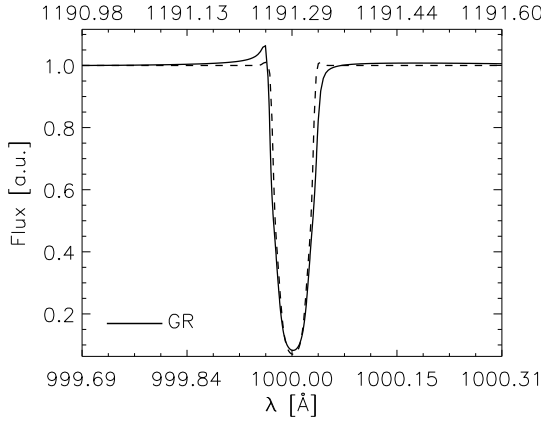


Fig. 4. The model line scatters with $\epsilon_{\text{line}} = 0.01$ while the continuum scattering factor is $\epsilon_{\kappa} = 1.0 \times 10^{-6}$.

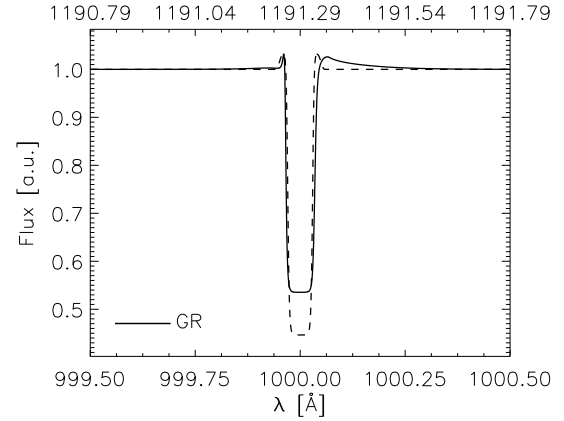


Fig. 5. The model line is nonscattering with a completely scattering – $\epsilon_{\kappa} = 0$ – continuum.

slope extends way farther into the blue, while on the red side of the line a very broad emission feature extends much farther to the red, although the peak is not as high as the blue peak. In addition, we have calculated a purely scattering ($\epsilon_{\text{line}} = 0$) model line combined with a purely absorptive continuum. This decouples the model line from the thermal pool. The results are shown in Fig. 6. Due to the scattering, the line is very strong, but the deformation of the lines wings is essentially the same as in Fig. 2, where the line did not scatter.

The effects of GR for the given atmosphere are most obvious for a scattering continuum. The resulting lineshape is strongly asymmetric. Scattering in the line has no discernible effect on the shape of the line. The actual deformation due to GR effects is also very small for pure linescattering.

The emergent lineshapes are related in principle to P-Cygni profiles, since there is also a constant wavelength shift – the dopplershift – throughout the atmosphere. However there is a fundamental difference between the two cases, since in an expanding atmosphere where P-Cygni profiles are observed there is a point of last contact of a photon with the atmosphere, hence the information of the dopplershift at the point of emission in respect to the observer is conserved. In the gravitational field the wavelength of the photon gets shifted even without any interaction with the atmosphere.

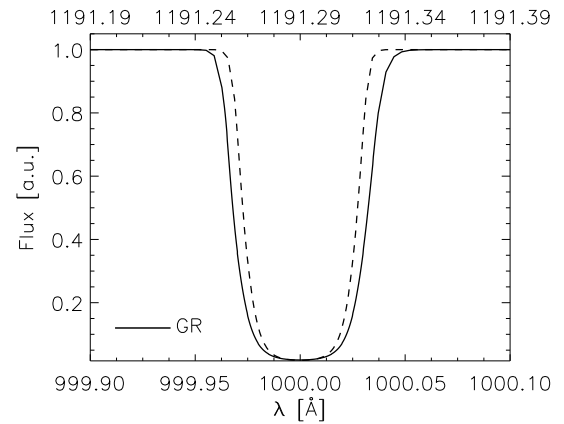


Fig. 6. The model line is completely scattering – $\epsilon_{\text{line}} = 0$ – while the continuum is not scattering at all.

5. Grey continuum models

As another application to general relativistic transfer we calculated grey continuum models. To do so we changed our wavelength resolution and omitted the model line from our calculations ($R_{\text{line}} = 0$). In the following we present the emerging continuous spectra for varying values of ϵ_{κ} .

The temperature structure of the model is grey with an effective temperature of 10^4 K (the absolute

value of the effective temperature is not important for the testing). The emergent spectra are nearly blackbody spectra with only a slightly distorted overall shape as they are a little bit broader than the blackbody.

To determine the effective temperature from an observation one would have to correct for the gravitational redshift and then try to fit a blackbody to the spectrum. This procedure will only deliver physically relevant results if the scattering conditions in the atmosphere are known. As long as all photons are absorbed and none scattered – $\epsilon_k = 1$ – (see Fig. 7) the emergent spectrum (corrected for gravitational redshift) is fitted with a blackbody with a temperature that is the same as the effective temperature of the model. For models with non-zero scattering – $\epsilon_k = 0.1$ in Fig. 8 and $\epsilon_k = 0.001$ in Fig. 10 – the emerging spectra are much bluer than the blackbody fit with the model effective temperature. In Fig. 9 and Fig. 11 we corrected the temperatures of the blackbody fits to match the emerging spectra. The apparent temperatures are much higher than the effective temperature of the model.

To prove the consistency of our results, we plot the thermalisation depth τ_{th} – the optical depth where the $J_\lambda = B_\lambda$ – over the scattering parameter ϵ_k . Since the emergent spectrum is Planckian, τ_{th} is the optical depth where the temperature of the atmosphere equals the temperature of the blackbody fit. The results are plotted in Fig. 12.

The results are consistent with the simple model $\tau_{th} = \frac{1}{\sqrt{\epsilon_k}}$. Hence, in the GR case the determination of effective temperatures via blackbody fits or simple radiative transfer models that neglect scattering will be inconsistent and result in systematic errors of the effective temperatures. Therefore, it is desirable to solve the scattering problem in a GR environment selfconsistently in a full blown atmospheric code with the method of solution that we present in this paper.

6. Conclusion

We have developed a method to solve continuum and line radiative transfer problems in spherically symmetric spacetimes that fully accounts for general relativistic effects and can account for scattering in the continuum and the lines. It uses a comoving frame wavelength formalism that allows resolution of spectral lines throughout the atmosphere without signif-

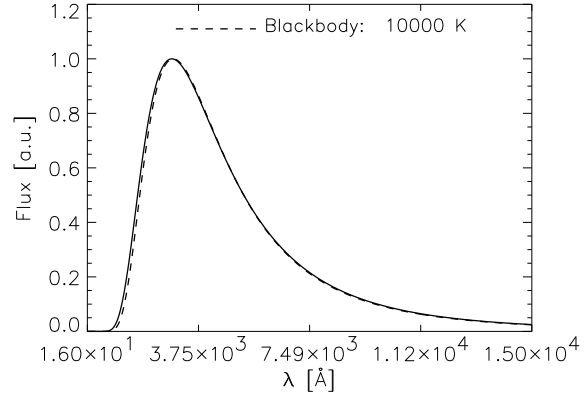


Fig. 7. The spectrum was corrected for the gravitational redshift and fitted with a blackbody with the known effective temperature of the model – $T_{eff} = 10^4$ K. The continuum has $\epsilon_k = 1$. The blackbody fits the model reasonably well.

icantly increasing the number of wavelength points. The method was developed and tested in static neutron star-like atmospheres, but is generally applicable to general relativistic systems. Only the photon orbits and the wavelength coupling term a_λ would be different in other GR systems. The test models provide an illustration of possible results for realistic model atmospheres for neutron stars. The results show that the emergent line profiles in general relativistic atmospheres cannot be described in detail with non-relativistic radiative transfer. The influence of the continuous scattering opacity on the shape of the lines is large.

The apparent effective temperature of continuous spectra also depends strongly on the strength of the scattering. Therefore, it is necessary to include the treatment of scattering in the radiative transfer solution in order to obtain a consistent physical model of a neutron star atmosphere and similar cases. The method that we have presented here is a first step to develop a thorough treatment of general relativistic atmosphere models in 3D. It can be directly applied to multi-level NLTE calculations of relativistic neutron star atmospheres, which we will present in a subsequent paper.

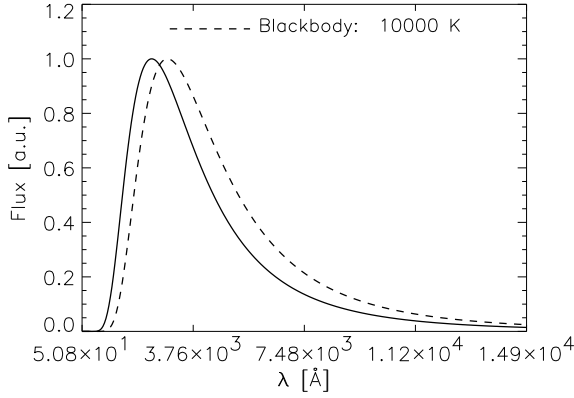


Fig. 8. The spectrum was corrected for the gravitational redshift and fitted with a blackbody with the known effective temperature of the model - $T_{\text{eff}} = 10^4$ K. The continuum has $\epsilon_k = 0.1$. The blackbody doesn't fit the model spectrum. The apparent temperature is higher than the model temperature.

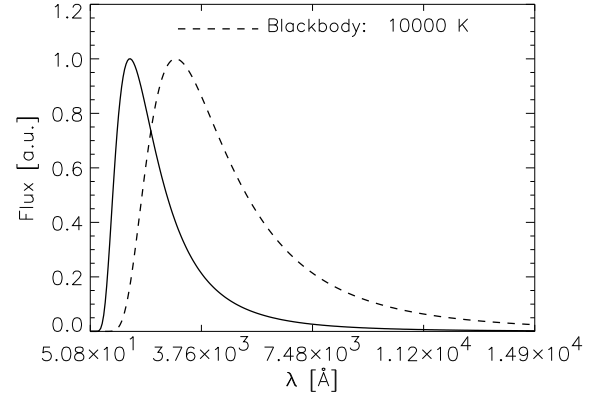


Fig. 10. The spectrum was corrected for the gravitational redshift and fitted with a blackbody with the known effective temperature of the model - $T_{\text{eff}} = 10^4$ K. The continuum has $\epsilon_k = 0.001$. The blackbody doesn't fit the model spectrum. The apparent temperature is higher than the model temperature.

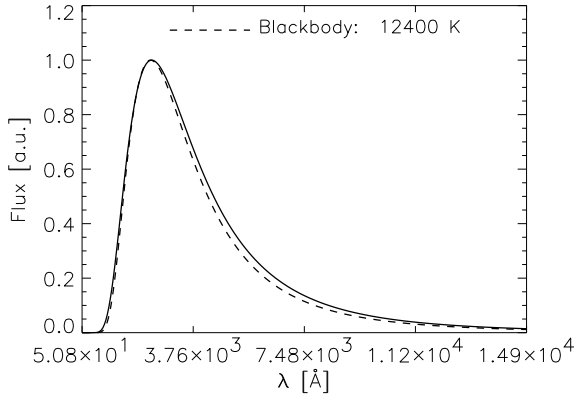


Fig. 9. The model spectrum is the same as in Figure 8, but this time the temperature of the blackbody was chosen to fit the spectrum.

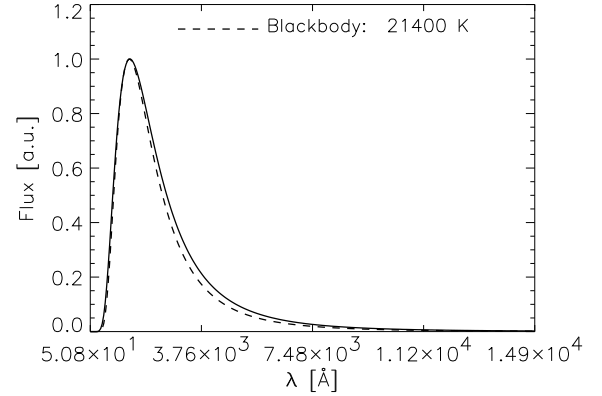


Fig. 11. The model spectrum is the same as in Figure 10, but this time the temperature of the blackbody was chosen to fit the spectrum.

References

- Baron, E. & Hauschildt, P. H. 2004, *A&A*, 427, 987
 Chandrasekhar, S. 1950, *Radiative transfer*. (Oxford, Clarendon Press, 1950.)

- Hauschildt, P. H., Starrfield, S., Shore, S. N., Allard, F., & Baron, E. 1995, *ApJ*, 447, 829
 Lindquist, R. 1966, *Annals of Physics*, 37, 487
 Mihalas, D. 1978, *Stellar atmospheres* /2nd edition/ (San Francisco, W. H. Freeman and Co., 1978. 650 p.)
 Mihalas, D. 1980, *ApJ*, 237, 574

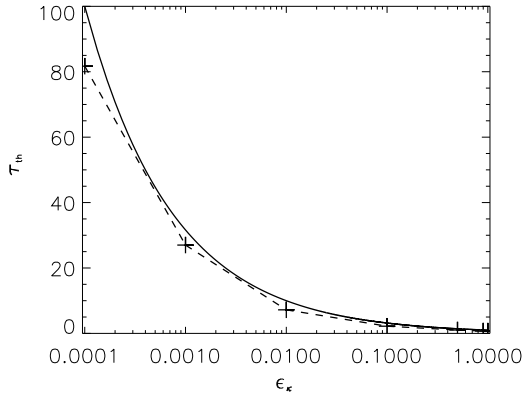


Fig. 12. Thermalisation depth is plotted over optical depth. Since the radial structure is only known on a discrete grid the value of the thermalisation depth for a given temperature was determined via linear interpolation.

Schinder, P. J. & Bludman, S. A. 1989, *ApJ*, 346, 350
 Zane, S., Turolla, R., Nobili, L., & Erna, M. 1996, *ApJ*, 466, 871
 Zavlin, V. E. & Pavlov, G. G. 2002, in *Neutron Stars, Pulsars, and Supernova Remnants*, ed. W. Becker, H. Lesch, & J. Trümper, 263–+